Optogenetic control of selective neural activity in multiple freely moving *Drosophila* adults

Ming-Chin Wu[a,1], Li-An Chu[b,1], Po-Yen Hsiao[b,1], Yen-Yin Lin[c,d,e], Chen-Chieh Chi[a], Tsung-Ho Liu[a], Chien-Chung Fu[a,c,f,2], and Ann-Shyn Chiang[b,c,g,h,2]

[a]Department of Power Mechanical Engineering, [b]Institute of Biotechnology, [c]Brain Research Center, [d]Institute of Photonics Technologies, [e]Department of Electrical Engineering, and [f]Institute of NanoEngineering and MicroSystems, National Tsing Hua University, Hsinchu 30013, Taiwan; [g]Genomics Research Center, Academia Sinica, Nankang, Taipei 11529, Taiwan; and [h]Kavli Institute for Brain and Mind, University of California, San Diego, La Jolla, CA 92093

Edited by Jeffrey C. Hall, University of Maine, Orono, ME, and approved February 25, 2014 (received for review January 24, 2014)

We present an automated laser tracking and optogenetic manipulation system (ALTOMS) for studying social memory in fruit flies (*Drosophila melanogaster*). ALTOMS comprises an intelligent central control module for high-speed fly behavior analysis and feedback laser scanning (~40 frames per second) for targeting two lasers (a 473-nm blue laser and a 593.5-nm yellow laser) independently on any specified body parts of two freely moving *Drosophila* adults. By using ALTOMS to monitor and compute the locations, orientations, wing postures, and relative distance between two flies in real time and using high-intensity laser irradiation as an aversive stimulus, this laser tracking system can be used for an operant conditioning assay in which a courting male quickly learns and forms a long-lasting memory to stay away from a freely moving virgin female. With the equipped lasers, channelrhodopsin-2 and/or halorhodopsin expressed in selected neurons can be triggered on the basis of interactive behaviors between two flies. Given its capacity for optogenetic manipulation to transiently and independently activate/inactivate selective neurons, ALTOMS offers opportunities to systematically map brain circuits that orchestrate specific *Drosophila* behaviors.

operant learning | restraining order | restraining conditioning

Social interactions are an important part of human life because they help us learn how to behave in a society. However, the mechanisms by which the neuron circuitry controls and modifies our behavior on the basis of previous experiences of interactions with others remain unclear. *Drosophila* courtship conditioning has been widely used for studying how genes and brain circuits control and modify a specific type of social interaction (1–6). In this behavioral assay, individual male fruit flies learn to suppress their courtship activity after several hours of exposure to an unreceptive female. Specific cuticular pheromones, such as 9-pentacosene, have been shown to potentially serve as conditioned stimuli (4, 7–9). Visual inputs act as conditioned stimuli for courtship through modulation of Ca^{2+}/calmodulin-dependent protein kinase activity in the brain circuitry (4). An aversive male pheromone, *cis*-vaccenyl acetate, which is transferred to the female during copulation, may act as a punishment so that the rejected male forms a generalized memory that suppresses its subsequent courtship behavior (10). However, little is known about where and how the neural activities that represent the antecedent conditions and aversive consequence are associated in the brain—knowledge that is crucial for understanding courtship memory and decision making—because controlling female rejection behaviors (11) and acutely manipulating target neurons in courting males during social interaction are difficult. Here, we present an automated laser tracking system for real-time analysis and perturbation of social interactions between two freely moving adult flies that is equipped with high-energy laser irradiation as a controllable punishment source to train a male during his interaction with a female fly.

Several automated systems have been designed to monitor the behaviors of freely moving flies through offline analysis (12–14) or to train restrained flies to respond to visual stimuli (15–17). Recent advances in the optogenetic manipulation of neural activity at the millisecond time scale by using light-activated channelrhodopsin-2 (ChR2) excitation or halorhodopsin (NpHR) inhibition have made it possible to study how neural circuits control behavior (18–23). Combining online image analysis and two lasers for acute punishment and optogenetic manipulation of selective neural activities, this automatic laser tracking and optogenetic manipulation system (ALTOMS) can precisely specify the timing of the purported associated events (antecedent conditions and response-dependent outcome), which could not be done in previous studies; this ability gives us better experimental control over courtship conditioning and an automated platform to systematically identify the neural circuits responsible for specific *Drosophila* behaviors.

Results

Hardware and Software. ALTOMS is an automated laser tracking system that comprises four parts: an image capture module (ICM), an intelligent central control module (ICCM), a laser scanning module (LSM), and a fly arena (Fig. 1 *A* and *B*; *SI Appendix*, Figs. S1 and S2). For real-time behavior analysis of multiple flies, we set a CCD camera in the ICM to record flies' movement at a resolution of 500 × 500 pixels per frame and a speed of 40

Significance

We present an automated laser tracking and optogenetic manipulation system (ALTOMS) for studying social memory in *Drosophila*. Based on behavioral interactions computed with a high-speed image analysis system, ALTOMS can target two lasers (a 473-nm blue laser and a 593.5-nm yellow laser) independently on any specified body parts of two freely moving *Drosophila* adults in real time. We performed an operant conditioning assay in which a courting male quickly learned and formed a long-lasting memory to stay away from a freely moving virgin female. Given its capacity for optogenetic manipulation to transiently and independently activate/inactivate selective neurons, ALTOMS offers opportunities to systematically map brain circuits that orchestrate specific *Drosophila* behaviors.

Author contributions: M.-C.W., L.-A.C., P.-Y.H., Y.-Y.L., C.-C.F., and A.-S.C. designed research; M.-C.W., L.-A.C., P.-Y.H., and C.-C.C. performed research; M.-C.W., L.-A.C., Y.-Y.L., and T.-H.L. contributed new reagents/analytic tools; M.-C.W., L.-A.C., P.-Y.H., Y.-Y.L., and A.-S.C. analyzed data; M.-C.W., L.-A.C., P.-Y.H., Y.-Y.L., C.-C.F., and A.-S.C. wrote the paper; and C.-C.F. and A.-S.C. supervised the project.

The authors declare no conflict of interest.

This article is a PNAS Direct Submission.

Freely available online through the PNAS open access option.

[1]M.-C.W., L.-A.C., and P.-Y.H. contributed equally to this work.

[2]To whom correspondence may be addressed. E-mail: ccfu@mx.nthu.edu.tw or aschiang@life.nthu.edu.tw.

This article contains supporting information online at www.pnas.org/lookup/suppl/doi:10.1073/pnas.1400997111/-/DCSupplemental.

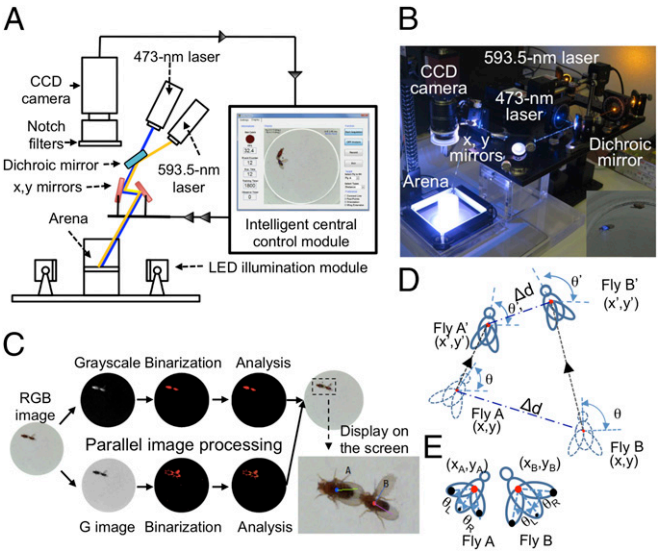

Fig. 1. Hardware and software for ALTOMS. (*A*) Schematic diagram of the setup. (*B*) Photograph of the setup. (*Inset*) Laser irradiation of one of two freely moving flies in the arena. (*C*) Steps involved in parallel processing from a single image to identifying the body center, orientation, relative distance between flies (top), and wing positions (bottom). (*Inset*) Calculated results displayed on the screen. (*D*) Tracking the movement of a fly by comparing the preposition (x, y) to the postposition (x′, y′). θ and θ′ denote the preorientation and postorientation, respectively, of the fly. The head and tail of each fly were defined according to the change in orientation of the animal. Δd denotes the relative distance between two flies. (*E*) The angles of wing extension for the left (θ_L) and right (θ_R) wings were computed automatically for each fly.

frames per second. To avoid interference during image acquisition for online image analysis, we placed two notch filters (473 ± 10 nm and 593.5 ± 10 nm) in front of the camera lens to selectively reject the laser lights (Fig. 1*A*). The acquired images were transferred immediately to the ICCM, which comprises online image analysis software developed using LabVIEW 2010 and a data acquisition device (*SI Appendix, SI Text*). The graphical user interface (GUI) of the ICCM offers options for online/offline analysis, experimental modes, hardware and software settings, and tools for laser calibration and data analysis (*SI Appendix,* Fig. S3). For example, the GUI settings for the distance restraining conditioning experiment (to be discussed later) include the to-be-targeted fly and the body part to be subjected to laser irradiation, training protocols, and testing parameters (*SI Appendix,* Fig. S4 and *SI Text*). To maximize the speed of online analysis, the ICCM uses a parallel image processing strategy (Fig. 1*C* and *SI Appendix,* Fig. S5). The system computes the following: the body position, orientation, and identity of each individual fly; the relative distance between two flies (Fig. 1*D* and *SI Appendix,* Fig. S5); and the angles of wing extension for the two flies (Fig. 1*E* and *SI Appendix* Fig. S5). Next, the ICCM automatically programs two sets of mechanical shutters and mirrors to determine the duration and position of laser irradiation (*SI Appendix, SI Text*).

For optogenetic manipulation, we used two diode-pumped solid-state lasers in the LSM: a 473-nm blue laser for ChR2 activation and a 593.5-nm yellow laser for NpHR inhibition. The minimal spatial and temporal resolutions of the LSM are 42 μm and 1 ms, respectively. The response time from image acquisition to laser irradiation is set to 25 ms. In the following sections, we demonstrate that ALTOMS is a versatile real-time behavior analysis/perturbation system that satisfies the requirements for studying complex behaviors between two freely fast-moving flies.

Position Tracking and Laser Irradiation. ALTOMS is capable of continuously tracking two fast-moving flies and changing the moving pattern of one by interactive laser irradiation without disturbing other flies in the same arena. To validate the effectiveness of laser tracking and irradiation, we performed a 10-min experiment during which a single fly moved freely in an arena that was virtually divided into two equal halves by the ICCM (Fig. 2*A*). The fly, which could not see this boundary, was irradiated continuously by a blue or yellow laser projected onto a specified body part (Fig. 2*B*) at several different energy levels whenever it entered the forbidden zone (left half of the arena). We found that flies rarely stayed in the forbidden zone when they were irradiated by either a blue (Fig. 2*C1*) or yellow (Fig. 2*C2*) laser over 20 mW/mm^2 in power on any body part. This avoidance response was laser intensity dependent. The highest "nonaversive" energy was 0.5 or 1 mW/mm^2 for blue laser targeting of the head/thorax or abdomen, respectively, and 7 mW/mm^2 for yellow laser targeting of any body part (Fig. 2*C*). By testing flies in a vertical 10-cm test tube, we showed that the climbing speed remained similar before and after laser irradiation in all cases (Fig. 2*D*), indicating that laser irradiation did not impair locomotion at any of the tested energies.

Next, we addressed whether laser irradiation of one fly affects the locomotion of another in the same arena and whether the irradiated fly associates the aversive laser irradiation with any environmental landmarks. We placed two flies in an arena for three consecutive 15-min sessions. During the first 15-min pretraining session, the two flies spent equal amounts of time in each of the two zones, indicating a lack of preference for either zone before the training session. Then, during the next 15-min training session, fly A was irradiated by a high-intensity blue laser (42 mW/mm^2) whenever it moved into the forbidden zone, whereas fly B was left undisturbed (Movie S1). Subsequently, fly A spent most of its time in the safe zone (right half of the arena),

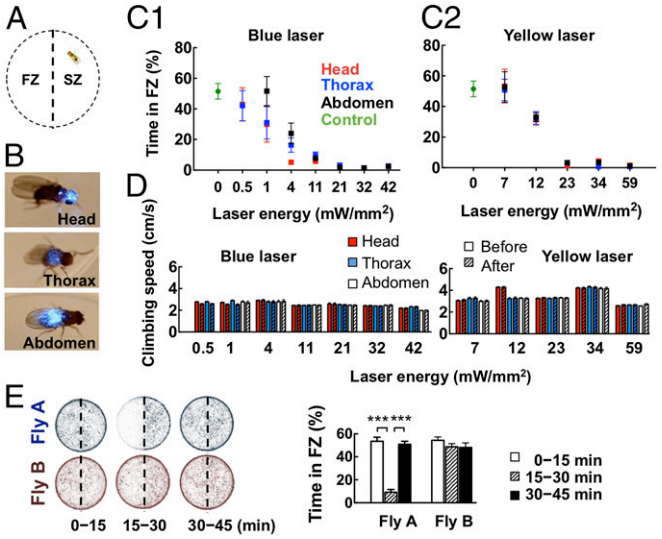

Fig. 2. Effectiveness of laser irradiation. (*A*) Virtual division of an arena into forbidden zone (FZ) and safe zone (SZ). (*B*) Laser targeting of three body parts: head, thorax, and abdomen. (*C*) Distribution of a male fly in the arena during 10-min blue (*C1*) or yellow (*C2*) laser irradiation at various energy levels. Each value represents mean ± SEM (n = 8). (*D*) Climbing speed in a 10-cm tube before and after laser irradiation of three different body parts. (*E*) Distributions of two male flies in the same arena during three consecutive 15-min sessions. The target male (fly A) was laser irradiated in the FZ (left half of arena) but not the SZ (right half of arena) during the second session but not the first and third sessions. The control male (fly B) was untouched in all sessions. (*Left*) Each dot represents the body position of a fly. (*Right*) Total time spent in the FZ during each session was determined. Each value represents mean ± SEM (n = 15), ***P < 0.001. Genotype: wild-type *Canton-S* w^{1118}.

whereas fly B spent equal amounts of time in each of the two zones (Fig. 2*E*). These results demonstrate that position tracking and laser irradiation are sufficiently fast and precise to effectively force a fly to change its locomotion pattern without disturbing another fly in the same arena. During the third 15-min post-training session without laser irradiation, fly A again spent equal amounts of time in each of the two zones, as did fly B. This observation indicates that fly A exhibited normal locomotion after laser irradiation and suggests that the arena setup did not provide sufficiently salient landmarks for fly A to associate laser punishment with a specific side of the arena.

The precision of tracking an identified male in real time is influenced by occasional crossover between two flies. Visual inspection of recorded videos (30 min for naïve flies and 60 min for trained flies) showed that the error rate for ALTOMS tracking was below 0.005% in all image frames (*SI Appendix*, Table S1).

Distance Restraining Conditioning. By using ALTOMS, we designed an operant learning paradigm in which a male fly was trained to follow an invisible "restraining order" by being punished upon violating the order. In this social learning assay, a naïve male instinctively attracted by a virgin female was punished by continuous high-intensity (42-mW/mm^2) blue laser irradiation (the aversive consequence) of the abdomen when he strayed within 3.5 mm of the female for more than 2 s (the antecedent condition) (Fig. 3*A*).

To determine whether ALTOMS reacts sufficiently fast for effective laser irradiation of the target, we measured the maximum distance a male fly could move within 25 ms (the time required for ALTOMS processing). The maximum moving speed of a male fly was 18.24 mm/s (13.69 mm/s on average) during training and 16.04 mm/s (11.71 mm/s on average) during the test (*SI Appendix*, Fig. S8*A*). Thus, during the 25-ms response time of the system, the maximum moving distance was 0.456 mm (0.34 mm on average), which still was covered by half the size of the laser spot (1.1 mm in diameter; *SI Appendix*, Fig. S8*B*). These measurements indicate that ALTOMS can effectively track two individual flies moving freely, compute their relative distance and angles of wing extension, and irradiate the laser beam at the selected target in time (Movie S2).

Next, we measured the restraining index (RI) after a 60-min restraining order training session by calculating the percentage of time a male stayed at least 3.5 mm away from a virgin female during a 30-min test period without laser irradiation. Naïve males often stayed near the virgin female (i.e., < 3.5 mm), but trained males rarely came close to the female even though they continued to move actively around the arena (Fig. 3 *B* and *C*). The duration and frequency of laser irradiation decreased gradually during the 60-min restraining conditioning session (Fig. 3*D*), suggesting that the male was learning to avoid the female during training. The energy level of laser irradiation also was critical for effective restraining order training. A male trained with a 42-mW/mm^2 laser avoided a virgin female at a significantly higher RI than a naïve male, although a male trained with a 21-mW/mm^2 laser exhibited an RI similar to that of a naïve male (Fig. 3*E*). To evaluate the chances of laser irradiation damage to the male fly's courtship ability and determine whether distance-irrelevant memory occurs during training, we designed two control experiments with a male subjected to pseudorandom laser irradiation in control group 1 (C1) and a male subjected to pseudorandom punishment in control group 2 (C2). The laser irradiation/punishment in both control groups was designed according to the actual 60-min operant distance restraining training session (Fig. 3*D* and *Materials and Methods*). Males in C1 groups courted normally and had an RI similar to that of a naïve male, suggesting that this laser irradiation protocol affects neither normal locomotion nor courtship behavior. Males in C2 groups had an RI similar to that of a naïve male, suggesting that an association between laser irradiation and distance to the female is critical for effective restraining order training (Fig. 3*E*).

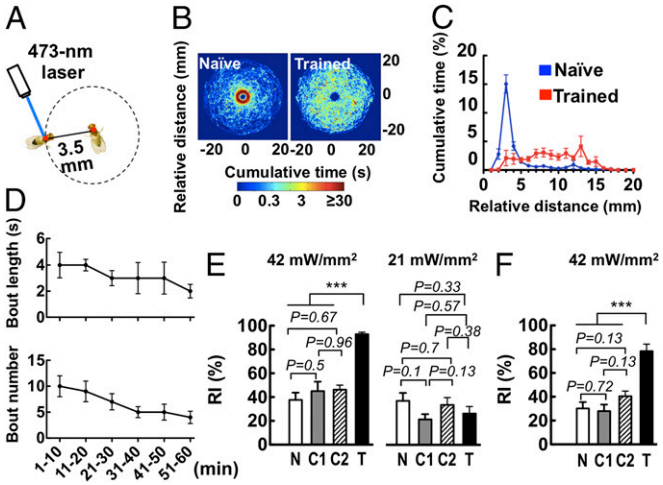

Fig. 3. Short-term and long-term operant distance restraining conditioning assay. (*A*) Schematic representation of a naïve male fly being irradiated whenever it strays within 3.5 mm of the female for more than 2 s. (*B*) Spatial distribution of a male around a freely moving virgin female during a 30-min test period. The male was either naïve or trained for 60 min before the test. Each pseudocolor image represents the results of 10 experiments accumulated by aligning the female's body position at the center origin. Color coding indicates the duration for which the males stayed at a given location. (*C*) Cumulative time across different ranges of relative distance between male and female during a 30-min test period after 60 min of training (n = 10). (*D*) Laser training bout length and bout number during a 60-min training session (n = 11). (*E*) RI of naïve (N), laser irradiation control (C1), pseudorandom punishment control (C2), and trained (T) groups during a 30-min test period after 60 min of training with 42-mW/mm^2 (*Left*) or 21-mW/mm^2 (*Right*) laser irradiation (n = 8). (*F*) RI of 24-h memory after training. In all experiments, each value represents mean ± SEM, ***P < 0.001. Genotype: wild-type *Canton-S* w^{1118}.

Operant Distance Restraining Conditioning Forms Long-Lasting Memory. *Drosophila* form long-lasting memories of conditioned courtship suppression when individual males are exposed for 5–7 h to an unreceptive female (3, 5, 24–28). In classical aversive olfactory conditioning, flies form long-lasting memories after ∼3 h of repetitive group training with spaced rest intervals (29, 30). Here, we found that after only 1 h of conditioning, individually trained males showed 24-h distance restraining memory. In contrast, control males subjected to pseudorandom laser irradiation or pseudorandom punishment did not exhibit significant 24-h memory (Fig. 3*F*). The strong and rapidly established memory suggests that a male fly perceives a freely moving female as an antecedent condition associated with the aversive consequence. In addition, ALTOMS can calculate the restraining distance and administer real-time laser irradiation as an effective punishment.

Trained Escape Behaviors. When encountering a virgin female during the test session, trained males exhibited four distinct escape responses: backward slipping, sideward sliding, jumping away, and/or turning and departing (Movie S3). Quantitative analysis of escape behaviors (*SI Appendix*, Fig. S9*A*) (31) indicated that these escape behaviors were observed frequently in trained males but rarely in naïve males or control males subjected to either pseudorandom laser irradiation or pseudorandom punishment (Fig. 4*A*). Automated offline analysis (*SI Appendix*, Fig. S9*B*) showed that trained males moved to a direction opposite the female's direction of approach (Fig. 4*B*). To test whether this male "distance-keeping phenomenon" varied with conditioning as a function of distance, we performed a modified distance restraining assay in a larger arena (*Materials and Methods*). We found that males conditioned at a distance of either 3.5 mm or 6 mm relative to the female exhibited similar escape behaviors when they encountered a virgin female during testing (*SI Appendix*, Fig. S9 *C*–*E*).

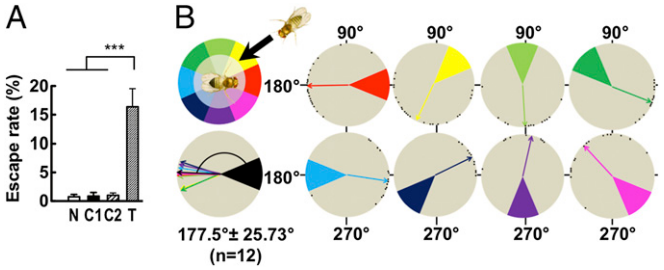

Fig. 4. Escape behaviors. (*A*) Escape rate of naïve (N), laser irradiation control (C1), pseudorandom punishment control (C2), and trained (T) males during a 30-min test period after 60 min of distance restraining training. Escape rate = escape bout/meeting bout. Each value represents mean ± SEM ($n = 8$), ***$P < 0.001$. (*B*) Quantitative analysis of male escape against female approach. The male was trained for an hour before testing with the same virgin female ($n = 12$). Each octant represented by a different color indicates a female's direction of approach. Black dots indicate the escape direction of individual males. Colored arrows indicate average male escape directions. Aligning 12 different datasets of female approach (black octant) and average male escape directions into one (black arrow) shows that trained males moved almost 180° against the female's direction of approach. Genotype: wild-type *Canton-S* w^{1118}.

Dual Optogenetic Manipulations. To interactively control selective neural activity depending on the social interactions between two flies, we equipped ALTOMS with two online lasers: a blue laser to activate ChR2-expressing neurons and a yellow laser to silence NpHR-expressing neurons. ChR2 is a widely used blue light-gated ion channel that contains the light-isomerizable chromophore all-*trans*-retinal for manipulating the electrical excitability of neurons (18, 32, 33). To demonstrate that ALTOMS was capable of photoactivating specific neurons within a living fly, we used *12862-Gal4* to drive ChR2 expression in the giant fiber neurons (Fig. 5*A*), a pair of brain interneurons that convey sensory information to the thoracic motor neurons and trigger the jumping reflex (34). We first tested the effectiveness of optogenetic ChR2 activation with the blue laser irradiated upon the head or thorax at different energy levels. When the laser energy was at or above 6 mW/mm^2, *12862-Ga4 > UAS-ChR2* flies fed with all-*trans*-retinal showed significantly higher rates of jumping than control flies without all-*trans*-retinal feeding or without *Gal4* to drive *ChR2* expression (Fig. 5*B* and Movie S4). Importantly, with the strongest blue laser (42 mW/mm^2), *12862-Ga4 > UAS-ChR2* flies fed with all-*trans*-retinal jumped frequently when the laser irradiated the head and thorax, where giant fibers are distributed, but not the abdomen (Fig. 5*C*), where giant fibers are absent (Fig. 5*A*). In all cases, control ChR2 flies without all-*trans*-retinal feeding rarely jumped (Fig. 5*C*). These results suggest that laser irradiation effectively triggers ChR2 on giant fibers and that the laser spot is sufficiently small and precise to target specific body parts during online tracking.

Next, we evaluated the effectiveness of optogenetic inhibition of neural activity in living flies with pan-neuronal expression of NpHR, which is a yellow light-driven pump specific for chloride ions (22, 35–37). With continuous yellow laser irradiation of the head or thorax, we found that experimental flies fed with all-*trans*-retinal exhibited an anesthesia rate positively correlated with laser energy and that most flies fainted after 60 s or 400 s laser irradiation at 34 or 23 mW/mm^2, respectively (Fig. 5*D*). In contrast, most control flies without all-*trans*-retinal feeding or without Gal4 to drive NpHR expression remained awake for at least 600 s after continuous irradiation at all tested laser energies (*SI Appendix*, Fig. S10). These results suggest that light-induced NpHR activity effectively silences the target neurons when the laser energy is greater than 23 mW/mm^2. The effectiveness decreased to zero when the energy fell below 5 mW/mm^2. All flies that had fainted awoke when the laser was turned off, suggesting that laser irradiation alone did not cause significant damage.

We also demonstrated that the jumping reflex is switched on/off rapidly by exciting and/or silencing giant fiber neurons that contained both ChR2 and NpHR by irradiating the head separately or simultaneously with a 21-mW/mm^2 blue laser and/or a 23-mW/mm^2 yellow laser (Fig. 5*E*). Whereas high jumping rates were triggered by optogenetic induction of ChR2 activation but not NpHR inhibition during all three 30-s sessions, simultaneous ChR2 activation and NpHR inhibition resulted in attenuated jumping rates. These results demonstrate that the two lasers in ALTOMS may be used separately or in combination to instantly and repetitively manipulate the activity of a target neuron within a specific body part of a freely moving fly.

Optogenetic Manipulation of Neural Circuits Delivering Punishment Signal. In contrast to traditional courtship conditioning assays, the operant distance restraining conditioning assay developed here used response-dependent irradiation with a strong laser as the aversive consequence of the antecedent condition instead of female rejection or aversive chemical cues. To fully appreciate the simplicity of a fly's operant learning, one must identify the neural circuits that process signals from both the antecedent conditions and consequent punishment. The gene products of *painless* are necessary for acute thermal nociception (38). *pain*^{1} is a *painless* mutant with P-element insertions upstream of the first noncoding exon and oriented in the same direction as the gene, resulting in the expression of mutant Painless proteins (38). We found that under our assay conditions, *pain*^{1} mutant males exhibited normal avoidance of high-intensity (42-mW/mm^2) blue laser irradiation (*SI Appendix*, Fig. S11) but had an RI similar to that of control flies immediately after training, suggesting that they failed to form short-term memory (Fig. 6*A*). *Pain-Gal4* is expressed in many neurons in both the brain and thoracic ganglia (Fig. 6*B*). By using a low-intensity blue laser (21 mW/mm^2) sufficient to activate ChR2 in giant fiber neurons (Fig. 5*B*) but insufficient to act as an aversive

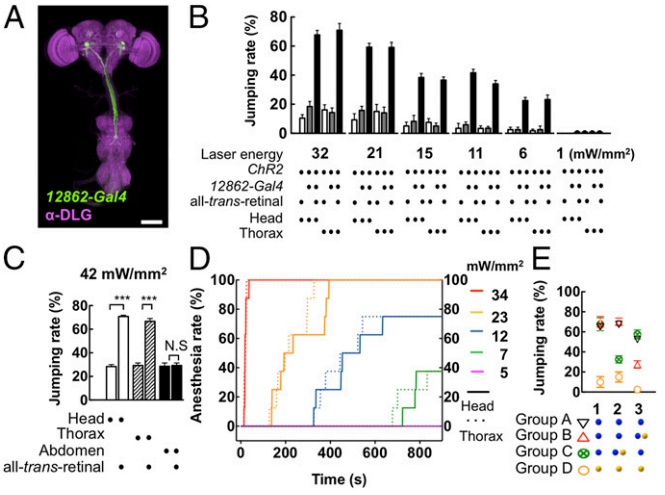

Fig. 5. Optogenetic manipulations. (*A*) Giant fiber neurons (green) were preferentially labeled in the *12862-Gal4 > UAS-GFP* fly. The brain and thoracic ganglia were immunostained with anti-discs large antibody (magenta). Scale bar represents 100 μm. (*B*) Jumping rates during 15 cycles of 3-s on-off blue laser irradiation on the head and thorax at different laser energies. (*C*) Jumping rates in *12862-Gal4>UAS-ChR2* flies under 42-mW/mm^2 laser irradiation of three different body parts. (*D*) Anesthesia rates as a function of time of continuous laser irradiation of the head or thorax at different energies in *Elav-Gal4/+;Gad-Gal4/UAS-eNpHR-YFP;nSyb-Gal4/UAS-eNpHR-YFP* flies. (*E*) Antagonistic effect between ChR2 activation and NpHR inhibition in *12862-Gal4/UAS-eNpHR-YFP;UAS-ChR2,UAS-eNpHR-YFP* flies. Four groups (A–D) of flies were irradiated by a 21-mW/mm^2 blue laser (blue dot) with or without a 23-mW/mm^2 yellow laser (yellow dot) on the head in three sequential experimental sessions (1–3). Each value represents mean ± SEM ($n = 8$), ***$P < 0.001$.

consequence in distance restraining conditioning (Fig. 3*E*, *Right*), we showed that activating ChR2 in thoracic *Pain-Gal4* neurons produced strong distance restraining memory (Fig. 6*C*) at a level equivalent to normal training with high-intensity (42-mW/mm^2) laser irradiation in wild-type flies without ChR2 expression (Fig. 3*E*, *Left*). In control experiments, distance restraining memory was not evident in flies with pseudorandom laser irradiation, with pseudorandom punishment, without retinal feeding, or without *Pain-Gal4* to drive ChR2 expression (Fig. 6*C*). These results suggest that ALTOMS effectively triggers target neurons at the right time, depending on the interactive behavior between two freely moving flies, and that optogenetic activation of *Pain-Gal4* neurons immediately following the antecedent conditions mimics the consequent punishment during operant distance restraining learning.

Discussion

ALTOMS is a fully automated and self-calibrating system that detects and computes the locations, orientations, wing postures, and relative distance of two freely fast-moving *Drosophila* adults online. Accordingly, the laser tracking module in ALTOMS can immediately irradiate specified body parts of a target fly. This interactive system incorporates several recent advances in automated behavior assay systems, including real-time interactive manipulation (16, 21, 39), wide-field observation of multiple individuals (12–14), and dual-color lasers for optogenetic manipulation (21). Real-time image analysis and laser tracking modules in ALTOMS offer several advantages: (*i*) high spatiotemporal precision of laser irradiation of specified body parts in a freely moving fly without disturbing another fly in the same arena, (*ii*) dual lasers for optogenetic activation or inhibition of selective neural activities simultaneously or separately (21, 40), (*iii*) a flexible and automated training program to manipulate neural circuits involved in courtship learning, and (*iv*) ready application to the study of other types of social behavior in flies. With the proper initial setup, the use of ALTOMS requires only minimal training without any special prior skills.

A caveat of the current ALTOMS setup is that flies avoid the strong light produced by a blue or yellow laser with an energy level above 0.5 mW/mm^2 (Fig. 2*C1*) or 7 mW/mm^2 (Fig. 2*C2*), respectively. Importantly, irradiation of a 1-mW/mm^2 blue laser from the dorsal surface was ineffective in activating ChR2 expressed on the ventrally located giant fibers (Fig. 5*B*), whereas a 7-mW/mm^2 yellow laser had only a partial effect in triggering pan-neuronal NpHR (Fig. 5*D*). These results suggest that optogenetic manipulation of giant fibers with an effective blue laser inevitably produces an aversive effect in the current ALTOMS setup. One potential way to prevent or at least minimize this unwanted side effect and improve the effectiveness of ChR2 activation of the giant fibers is to change the direction of laser irradiation from dorsal to ventral, because a 0.5-mW/mm^2 laser has been shown to be effective for optogenetic manipulation of peripheral neurons (41). Alternatively, a red-shifted ChR2 activated by a longer-wavelength laser to which flies are blind will be helpful (42, 43). These changes also may improve the effectiveness of NpHR inhibition.

A restraining order or "order of protection" is a form of legal injunction that requires a party to refrain from performing certain acts; refusal to comply invites some form of punishment. By using high-intensity laser irradiation as a punitive stimulus, we showed that a courting male quickly learns to avoid punishment by staying a minimum distance away from a freely moving virgin female and forms a long-lasting memory that lasts at least 24 h. The "distance restraining conditioning" established here is a form of operant learning in which a single male learns the association between an antecedent condition (i.e., the decision to stay within a fixed distance of a freely moving female) and an aversive consequence (i.e., response-dependent irradiation with a strong laser), the frequency and duration of which gradually decrease during training (Fig. 3*D*). Rapid recovery in the forbidden zone assay (Fig. 2*E*) indicated that the male may learn the distance restraining order without visual knowledge of geographic landmarks. Although flies avoided visible lasers at high energy (Fig. 2*C*), our results indicate that avoidance under 21 mW/mm^2 was unrelated to restraining conditioning (Figs. 2*C* and 3*E*, *Right*). Finally, similar to artificial activation of dopaminergic neurons projecting to the mushroom body that mimic the unconditioned stimulus in classical olfactory associative learning (20) and traditional courtship learning (6), we found that ChR2 activation of *Pain-Gal4* neurons mimics the aversive consequence in operant distance restraining learning (Fig. 6*C*) and that normal expression of *painless* gene products is necessary for the formation of distance restraining memory (Fig. 6*A*). It would be interesting to know whether there are dopaminergic neurons downstream of the *painless* neurons to associate the aversive consequence with the antecedent conditions in the operant distance restraining learning assay developed here. With its capacity for optogenetic manipulation to acutely and independently turn on/off neuronal activities, ALTOMS offers opportunities to systematically map memory circuits in the *Drosophila* brain.

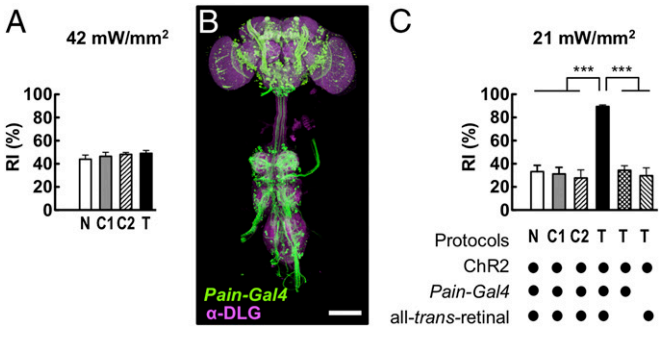

Fig. 6. Neural circuitry of laser punishment. (*A*) RI of short-term memory immediately after training in *pain*^{1} mutant males. During training, a strong blue laser (42 mW/mm^2) was used to irradiate the abdomen of naïve (N), laser irradiation control (C1), pseudorandom punishment control (C2), and trained (T) male flies. (*B*) The expression pattern of *Pain-Gal4*. (*C*) Laser punishment mimicked by activating *Pain-Gal4* neurons. *Pain-Gal4* > *UAS-ChR2* flies were fed with or without all-*trans*-retinal in the food for 5–7 d. Blue laser was irradiated on the thorax. In all experiments, each value represents mean ± SEM (n = 8), ***P < 0.001.

Materials and Methods

Fly Strains. Fly stocks were maintained on standard cornmeal/yeast/agar medium at 25 ± 1 °C and 70% relative humidity on a 12:12-h light:dark cycle. For the distance restraining conditioning assays, each male fly was housed singly from the pupal stage. For optogenetic experiments, the male was kept in a standard fly medium containing 100 μM all-*trans*-retinal for 5–7 d before the assay. The following fly stocks were used in the study: *UAS-ChR2* (from Klemens F. Störtkuhl, Georg-August-University of Goettingen, Goettingen, Germany); *UAS-NpHR-eYFP* (from Akinao Nose, University of Tokyo, Tokyo); *Pain1* [EP(2)2452] and *Pain-Gal4* (from Zuoren Wang, Shanghai Institutes for Biological Sciences, Shanghai, China); and *Elav-Gal4*, *Gad-Gal4*, *nSyb-Gal4*, *12862-Gal4*, and wild-type flies *Canton-S w*^{1118} (iso1CJ) (from the Bloomington Stock Center). All behavioral assays were carried out at 25 ± 1 °C and 40% relative humidity.

Distance Restraining Conditioning. A mature adult male instinctively is attracted toward a mature virgin female. We kept a 7-d-old naïve male with a virgin female in an arena 20 mm in diameter and trained the male to behave against this strong innate behavior by punishing him whenever he was close to the virgin female. All males used in this assay were housed singly from the pupal stage. During a 60-min training period, we used a strong blue laser (42 mW/mm^2) to irradiate the male's abdomen when the distance between the two flies was shorter than 3.5 mm (approximately equal to the female's body length) for more than 2 s (Fig. 3*A*). We used 2 s as a filter so that the male was not punished merely for passing by the female. We measured the RI after a 60-min distance restraining training session by calculating the percentage of time a male stayed at least 3.5 mm away from a virgin female during a 30-min test period without laser irradiation. The trained male (T)

was considered to have distance restraining memory only if its RI was significantly higher than all three independent sham-control males: naïve (N), pseudorandom laser irradiation (C1), and pseudorandom punishment (C2). In the case of N (a male kept separately in an arena for 60 min without laser irradiation) and C1 (a male kept separately in an arena for 60 min with pseudorandom laser irradiation), the male's RI was determined immediately by introducing a naïve virgin female into the arena for 30 min. In the case of C2 (a male kept with a virgin female in the same arena that was pseudorandomly punished by laser irradiation for 60 min when the two flies were more than 3.5 mm apart), pseudorandom training was aborted if the two flies mated. The male's RI then was tested with the same female for 30 min. The protocols for pseudorandom irradiation/punishment were designed according to the actual 60-min operant distance restraining training session. During this period, the duration and frequency of laser irradiation decreased gradually (Fig. 3*D*): 1–10 min, 4 s per 10 times; 11–20 min, 4 s per 9 times; 21–30 min, 3 s per 7 times; 31–40 min, 3 s per 5 times; 41–50 min, 3 s per 5 times; and 51–60 min, 2 s per 4 times.

Optogenetic Manipulation. We used a blue laser (473 nm) to activate ChR2 and a yellow laser (593.5 nm) to activate NpHR. The ALTOMS system automatically controlled the laser so that it always repetitively irradiated the same target (head, thorax, or abdomen) of a freely moving fly during the test. For the ChR2-induced jumping experiment, the laser irradiation was 15 cycles with a 3-s on/off interval. For the experiment combining ChR2 and NpHR, each group of flies was subjected to three consecutive sessions of 30-s laser irradiation. Each session contained five cycles of 3-s on/off laser irradiation at different combinations. Flies in group A were subjected to 21-mW/mm^2 blue laser irradiation for all three sessions. Flies in group B were treated in the same manner as those in group A with the exception of simultaneous 23-mW/mm^2 yellow laser irradiation during session 2. Flies in group C also were treated in the same manner as those in group A with the exception of simultaneous 23-mW/mm^2 yellow laser irradiation during session 3. Flies in group D were subjected to 23-mW/mm^2 yellow laser irradiation for all three sessions.

Anesthesia Assay. Flies were fed a standard food medium with or without 100 μM all-*trans*-retinal for 5–7 d before the experiment. Following retinal feeding, experimental flies carrying *Elav-Gal4/+;Gad-Gal4/UAS-eNpHR-YFP; nSyb-Gal4/UAS-eNpHR-YFP* transgenes were irradiated continuously on the head by a yellow laser (593.5 nm) for 15 min. Control flies carrying *UAS-eNpHR-YFP/+;UAS-eNpHR-YFP/+* transgenes with retinal feeding or *Elav-Gal4/+;Gad-Gal4/UAS-eNpHR-YFP;nSyb-Gal4/UAS-eNpHR-YFP* transgenes without retinal feeding were subjected to the same laser irradiation treatment.

Statistical Analysis. Significantly different groups were compared pairwise by the two-tailed Mann–Whitney test.

ACKNOWLEDGMENTS. We thank Klemens F. Störtkuhl, Akinao Nose, Zuoren Wang, and the Bloomington Stock Center for providing flies. We thank Tsai-Feng Fu and Chih-Wei Hsu for initial tests on optogenetic experiments. We thank An-Kuo Hong for initial tests on distance restraining conditioning. We also thank National Instruments, NI Taiwan. We thank Hsiu-Ming Chang, Tsung-Pin Pai, and Cheng-Wen Huang for discussions and comments. This work was supported by grants from the National Science Council and the Aim for the Top University Project of the Brain Research Center at National Tsing Hua University and the Ministry of Education, and a Distinguished Scholar Research grant from the National Science Council in Taiwan.

1. Siegel RW, Hall JC (1979) Conditioned responses in courtship behavior of normal and mutant *Drosophila*. *Proc Natl Acad Sci USA* 76(7):3430–3434.
2. Gailey DA, Jackson FR, Siegel RW (1984) Conditioning mutations in *Drosophila melanogaster* affect an experience-dependent behavioral modification in courting males. *Genetics* 106(4):613–623.
3. McBride SM, et al. (1999) Mushroom body ablation impairs short-term memory and long-term memory of courtship conditioning in *Drosophila melanogaster*. *Neuron* 24(4):967–977.
4. Joiner MA, Griffith LC (2000) Visual input regulates circuit configuration in courtship conditioning of *Drosophila melanogaster*. *Learn Mem* 7(1):32–42.
5. Griffith LC, Ejima A (2009) Courtship learning in *Drosophila melanogaster*: Diverse plasticity of a reproductive behavior. *Learn Mem* 16(12):743–750.
6. Keleman K, et al. (2012) Dopamine neurons modulate pheromone responses in *Drosophila* courtship learning. *Nature* 489(7414):145–149.
7. Tompkins L, Siegel RW, Gailey DA, Hall JC (1983) Conditioned courtship in *Drosophila* and its mediation by association of chemical cues. *Behav Genet* 13(6):565–578.
8. Ejima A, Smith BP, Lucas C, Levine JD, Griffith LC (2005) Sequential learning of pheromonal cues modulates memory consolidation in trainer-specific associative courtship conditioning. *Curr Biol* 15(3):194–206.
9. Siwicki KK, et al. (2005) The role of cuticular pheromones in courtship conditioning of *Drosophila* males. *Learn Mem* 12(6):636–645.
10. Ejima A, et al. (2007) Generalization of courtship learning in *Drosophila* is mediated by *cis*-vaccenyl acetate. *Curr Biol* 17(7):599–605.
11. Connolly K, Cook R (1973) Rejection responses by female *Drosophila-melanogaster*—their ontogeny, causality and effects upon behavior of courting male. *Behaviour* 44(1-2):142–166.
12. Dankert H, Wang L, Hoopfer ED, Anderson DJ, Perona P (2009) Automated monitoring and analysis of social behavior in *Drosophila*. *Nat Methods* 6(4):297–303.
13. Branson K, Robie AA, Bender J, Perona P, Dickinson MH (2009) High-throughput ethomics in large groups of *Drosophila*. *Nat Methods* 6(6):451–457.
14. Ofstad TA, Zuker CS, Reiser MB (2011) Visual place learning in *Drosophila melanogaster*. *Nature* 474(7350):204–207.
15. Xia S, Liu L, Feng C, Guo A (1997) Memory consolidation in *Drosophila* operant visual learning. *Learn Mem* 4(2):205–218.
16. Liu L, Wolf R, Ernst R, Heisenberg M (1999) Context generalization in *Drosophila* visual learning requires the mushroom bodies. *Nature* 400(6746):753–756.
17. Pan Y, et al. (2009) Differential roles of the fan-shaped body and the ellipsoid body in *Drosophila* visual pattern memory. *Learn Mem* 16(5):289–295.
18. Zhang W, Ge W, Wang Z (2007) A toolbox for light control of *Drosophila* behaviors through Channelrhodopsin 2-mediated photoactivation of targeted neurons. *Eur J Neurosci* 26(9):2405–2416.
19. Clyne JD, Miesenböck G (2008) Sex-specific control and tuning of the pattern generator for courtship song in *Drosophila*. *Cell* 133(2):354–363.
20. Claridge-Chang A, et al. (2009) Writing memories with light-addressable reinforcement circuitry. *Cell* 139(2):405–415.
21. Leifer AM, Fang-Yen C, Gershow M, Alkema MJ, Samuel AD (2011) Optogenetic manipulation of neural activity in freely moving *Caenorhabditis elegans*. *Nat Methods* 8(2):147–152.
22. Inada K, Kohsaka H, Takasu E, Matsunaga T, Nose A (2011) Optical dissection of neural circuits responsible for *Drosophila* larval locomotion with halorhodopsin. *PLoS One* 6(12):e29019.
23. Zhao S, et al. (2011) Cell type–specific channelrhodopsin-2 transgenic mice for optogenetic dissection of neural circuitry function. *Nat Methods* 8(9):745–752.
24. Kamyshev NG, Iliadi KG, Bragina JV (1999) *Drosophila* conditioned courtship: Two ways of testing memory. *Learn Mem* 6(1):1–20.
25. Keleman K, Krüttner S, Alenius M, Dickson BJ (2007) Function of the *Drosophila* CPEB protein Orb2 in long-term courtship memory. *Nat Neurosci* 10(12):1587–1593.
26. Ishimoto H, Sakai T, Kitamoto T (2009) Ecdysone signaling regulates the formation of long-term courtship memory in adult *Drosophila melanogaster*. *Proc Natl Acad Sci USA* 106(15):6381–6386.
27. Fitzsimons HL, Scott MJ (2011) Genetic modulation of Rpd3 expression impairs long-term courtship memory in *Drosophila*. *PLoS One* 6(12):e29171.
28. Winbush A, et al. (2012) Identification of gene expression changes associated with long-term memory of courtship rejection in *Drosophila* males. *G3 (Bethesda)* 2(11): 1437–1445.
29. Tully T, Quinn WG (1985) Classical conditioning and retention in normal and mutant *Drosophila melanogaster*. *J Comp Physiol A Neuroethol Sens Neural Behav Physiol* 157(2):263–277.
30. Chen CC, et al. (2012) Visualizing long-term memory formation in two neurons of the *Drosophila* brain. *Science* 335(6069):678–685.
31. Card G, Dickinson MH (2008) Visually mediated motor planning in the escape response of *Drosophila*. *Curr Biol* 18(17):1300–1307.
32. Boyden ES, Zhang F, Bamberg E, Nagel G, Deisseroth K (2005) Millisecond-timescale, genetically targeted optical control of neural activity. *Nat Neurosci* 8(9):1263–1268.
33. Zhang YP, Oertner TG (2007) Optical induction of synaptic plasticity using a light-sensitive channel. *Nat Methods* 4(2):139–141.
34. Lima SQ, Miesenböck G (2005) Remote control of behavior through genetically targeted photostimulation of neurons. *Cell* 121(1):141–152.
35. Zhang F, et al. (2007) Multimodal fast optical interrogation of neural circuitry. *Nature* 446(7136):633–639.
36. Han X, Boyden ES (2007) Multiple-color optical activation, silencing, and desynchronization of neural activity, with single-spike temporal resolution. *PLoS One* 2(3):e299.
37. Gradinaru V, et al. (2010) Molecular and cellular approaches for diversifying and extending optogenetics. *Cell* 141(1):154–165.
38. Tracey WD, Jr., Wilson RI, Laurent G, Benzer S (2003) *painless*, a *Drosophila* gene essential for nociception. *Cell* 113(2):261–273.
39. Seelig JD, Jayaraman V (2011) Studying sensorimotor processing with physiology in behaving *Drosophila*. *Int Rev Neurobiol* 99:169–189.
40. Zhu P, Fajardo O, Shum J, Zhang Schärer YP, Friedrich RW (2012) High-resolution optical control of spatiotemporal neuronal activity patterns in zebrafish using a digital micromirror device. *Nat Protoc* 7(7):1410–1425.
41. Suh GS, et al. (2007) Light activation of an innate olfactory avoidance response in *Drosophila*. *Curr Biol* 17(10):905–908.
42. Lin JY, Knutsen PM, Muller A, Kleinfeld D, Tsien RY (2013) ReaChR: A red-shifted variant of channelrhodopsin enables deep transcranial optogenetic excitation. *Nat Neurosci* 16(10):1499–1508.
43. Inagaki HK, et al. (2014) Optogenetic control of *Drosophila* using a red-shifted channelrhodopsin reveals experience-dependent influences on courtship. *Nat Methods* 11(3):325–332.

Supplementary Information

Wu et al.

SI Text

System apparatus. ALTOMS for behavioral training of flies comprises four modules: an arena, an image capture module (ICM), a laser scanning module (LSM), and an intelligent central control module (ICCM) (Fig. S1).

Arena. The arena was made of acrylic materials, and consisted of an upper arena and a supporting base (Fig. S2). The center of the upper arena contained a behavioral chamber that was 20 mm in diameter and 3 mm in height. To keep the flies standing on the floor, the walls and cover of the chamber are coated with Fluon (Kingtec$^{@\,TW}$) and water repellent (Rain-X^{R}), respectively. This design forces the flies to remain on the floor during the experiment. The supporting base helps to provide even light illumination for better image quality.

ICM. The ICM consists of two parts: a charge-coupled device (CCD) camera (AVT^{TM} Pike F-100C from Allied Vision Technologies Corp.) and a white light-emitting diode (LED) illumination module (EXLITE DAL-15-100-4-W from EXLITE Technology Co.). For distance-restraining conditioning, we set the aperture of the CCD lens (FUJINON HF-35SA-1) at F5.6 and the camera taping rate at 500 × 500 pixels/frame and 40 fps. The obtained image of 25 × 25 pixels/mm^2 provides a suitable spatial resolution for detailed analysis of fly behavior.

LSM. The characteristics of high intensity and low divergence make a laser beam a suitable light resource for illuminating a selected fly without affecting other flies nearby. The LSM consisted of two surface mirrors steered by Galvo motors (GSI VM500+) for simultaneously or separately guiding a blue laser (wavelength: 473 nm; maximum intensity: 42 mW/mm^2) and/or a yellow laser (wavelength: 593.5 nm; maximum intensity: 59 mW/mm^2). The laser spot sizes measured by a beam profiler (DataRay Inc. BladeCam-HR CMOS Camera) were 1.1 mm and 1.05 mm in diameter for the 473-nm and 593.5-nm lasers, respectively (Fig. S8B). A dichroic mirror (reflection band: 380–490 nm; transmission band: 520–700 nm) was used to combine two different lasers. Two independent mechanical shutters (Thorlabs, Inc. SH05; aperture: 12.7 mm; minimum exposure time: ≈1 ms) were used to switch each laser beam on/off independently. The other mirrors were broadband high-reflectivity dielectric mirrors (Thorlabs, Inc. BB1-E02 400–740 nm). The LSM response time was ~1 ms.

ICCM. The operation of the ICCM is explained on the basis of the (1) graphical user interface (GUI), (2) image processing, (3) laser calibration, and (4) algorithm flowchart.

(1) GUI. The GUI developed for users to program the experiment includes the following components (Fig. S3):

(**a**) "Source" is used to select the type of analysis (online mode from CCD camera or offline mode from pre-captured video).
(**b**) "Mode" is used to select the type of experiment (forbidden zone or distance-restraining conditioning).
(**c**) "Hardware" sets up the path to load the videotaped image (for offline analysis only, if necessary), communication port of the "data acquisition" device (DAQ, National Instruments, to control the X-Y Galvo motors), two shutters, and error warning for system malfunctions.
(**d**) "Software" specifies the information, preference, display, system, and training protocol for the distance-restraining conditioning assay (Fig. S4). The information function shows the status of the system, including "Not catch," which indicates failure to distinguish between 2 flies with a red-light warning; "FPS," which indicates the number of frames per second; "Encounter time," which indicates the time accumulated within the restraining distance; and "Timer," which counts the progress of the assay. The preference function provides options to display "Connect line," which indicates the distance between 2 flies, "Past points," which indicates traces of previous locations, "Orientation," and "Wing extension angle." The display panel shows an image of two labeled flies (center), angles of wing extension for the target fly (upper left), distance between the two flies (upper right), and laser on-off indication. The system provides the options of "Continuous" (for adjusting the system without recording), "Off," "Record," and "Exit." The training protocol provides options to set the "Training length" (3600 s in this study), "Test length" (1800 s in this study), "Fly" (Fly-A or Fly-B), "Target" (head, thorax, or abdomen for laser irradiation), and "Conditioned stimulus" (laser irradiation based on distance between flies or angles of wing extension for the target fly).
(**e**) "Laser calibration" (see below).
(**f**) "Data analysis": The output data include the distance between two flies at each second, time point at which two flies encounter each other (D), time point at which the male fly extends its wing (WE), longest/shortest/average/total meeting period (LMP/SMP/AMP/TMP), meeting bout number, wing extension period (WEP), wing extension bout number (WE Bout), and average distance.

(2) Image processing. We have developed an automated tracking system to track the movement of multiple individual flies. The results of behavior analysis indicate that the system is capable of interactively irradiating the target fly in real time with a laser. To maximize the speed of online analysis, we adopted a parallel image processing strategy (Fig. S5).

(**a**) **Detection of fly positions.** To facilitate image processing, we first converted the color image of flies in the arena into a gray level image. Next, we obtained information about the morphology of the fly body from the extracted saturation plane (S) of the image[43].

$$S = 1 - \frac{3}{(R+G+B)}[\min(R,G,B)] \quad (1)$$

After applying a suitable long-pass threshold value, the gray level image was then converted into a binary image. Next, we obtained the complete fly contours by applying the "Morphology Closing" image processing function that smoothed the contours, filled small holes within the fly bodies, and eliminated small particles outside the fly bodies.

$$A \cdot B = (A \oplus B) \ominus B \quad (2)$$

Here, $\oplus$ and $\ominus$ denote the dilation and erosion, respectively.

We then applied "Area" as a noise filter to remove large particles other than fly bodies. Finally, we calculated the center point of the fly mass and overlaid the result on the image.

$$\bar{x} = \frac{\sum_x \sum_y xf(x,y)}{\sum_x \sum_y f(x,y)} \qquad \bar{y} = \frac{\sum_x \sum_y yf(x,y)}{\sum_x \sum_y f(x,y)} \quad (3)$$

Here, x and y represent the pixel's position and f(x, y) represents the pixel's value.

(**b**) **Detection of angles of wing extension.** Angles of wing extension and the positions of two freely moving flies were determined in parallel (Fig. S5). After converting the gray level image into a binary image, we applied the "Band Thresholding" and "Morphology Erosion" functions to extract wing structures.

$$A \ominus B = \bigcap_{b \in B} A_{-b} \quad (4)$$

Here, B is a structuring element.

Finally, after removing small particles by using the "Area" noise filter, we specified a range of diameter values for automatic detection of wing positions[44].

(**c**) **Recognition of fly identity.** In addition to the positions of flies and wings, several other parameters were also obtained (i.e., orientation, distance between two flies, positions of head and tail for each fly). Next, we used the nearest distance method to track a target fly. For example, the position of one of two flies in the current frame "P_t" was compared with the position of Fly-A or Fly-B in the previous frame "P_{t-1}"[45].

$$Fly_{id} = \text{nearest distance } (P_t - P_{t-1}) \quad (5)$$

The one near Fly-A was assigned as the new position of Fly-A. The same holds for Fly-B.

The fly movements (e.g., quick turn, roll, and jump) were abrupt and unpredictable. To avoid judgment errors, our program also compared the positions of the flies' head and tail with respect to the orientations in consecutive frames.

$$Fly_{orientation} = \theta_t - \theta_{t-1} \quad (6)$$

where θ_{t-1} is the orientation in frame t–1 and θ_t, the orientation in frame t. The program automatically added or subtracted 180° when the discrepancy between the t–1 and t frames exceeded 180°.

The nearest distance was also used to match the detected wings and identified flies. Our program calculated the mutual distances of all the available wing positions and bundled the nearest two wings to the same fly. The angle of wing extension was calculated for each wing by comparing the body axis to the line linking the wing mass center and the body mass center (Fig. S5). The resolution to estimate this angle was set at 15°, which was also difficult for visual inspection. A fly with an angle of wing extension below 15° was considered to be in a resting position.

In our system, the total time required from image acquisition to laser irradiation for the selected fly was 25 ms, including approximately 24 ms for image analysis and 1 ms for LSM processing. The maximal operation speed was ~40 fps.

(3) Laser calibration. Calibrating the spatial precision of laser irradiation before starting an experiment is crucial (Fig. S3E). To visualize the location of laser irradiation, we additionally placed a special acrylic fluorescence plate at the bottom of the behavior chamber (Fig. S6A1). A spot irradiated by the blue laser on the white acrylic plate emitted green fluorescence (Fig. S6A2). After color thresholding and particle filtering, the center point of the laser spot was calculated (Fig. S6A3). Laser positioning was calibrated 5 times by matching the laser-induced fluorescence spots to five fixed points on the fluorescence plate via manual inputs of different voltage signals (Fig. S6B). We have created a lookup table to calibrate the relative coordinates between the scanner and the specified locations on the arena.

(4) Algorithm flowchart. For an overview of ALTOMS, an algorithm flowchart is provided (Fig. S7).

1. Siegel RW & Hall JC (1979) Conditioned responses in courtship behavior of normal and mutant *Drosophila*. *Proc Natl Acad Sci U S A* 76(7):3430-3434.
2. Gailey DA, Jackson FR, & Siegel RW (1984) Conditioning mutations in *Drosophila melanogaster* affect an experience-dependent behavioral modification in courting males. *Genetics* 106(4):613-623.
3. McBride SM, *et al.* (1999) Mushroom body ablation impairs short-term memory and long-term memory of courtship conditioning in *Drosophila melanogaster*. *Neuron* 24(4):967-977.
4. Joiner MA & Griffith LC (2000) Visual input regulates circuit configuration in courtship conditioning of *Drosophila melanogaster*. *Learn Mem* 7(1):32-42.
5. Griffith LC & Ejima A (2009) Courtship learning in *Drosophila melanogaster*: diverse plasticity of a reproductive behavior. *Learn Mem* 16(12):743-750.
6. Keleman K, *et al.* (2012) Dopamine neurons modulate pheromone responses in *Drosophila* courtship learning. *Nature* 489(7414):145-149.
7. Tompkins L, Siegel RW, Gailey DA, & Hall JC (1983) Conditioned courtship in *Drosophila* and its mediation by association of chemical cues. *Behav Genet* 13(6):565-578.
8. Ejima A, Smith BP, Lucas C, Levine JD, & Griffith LC (2005) Sequential learning of pheromonal cues modulates memory consolidation in trainer-specific associative courtship conditioning. *Curr Biol* 15(3):194-206.
9. Siwicki KK, *et al.* (2005) The role of cuticular pheromones in courtship conditioning of *Drosophila* males. *Learn Mem* 12(6):636-645.
10. Ejima A, *et al.* (2007) Generalization of courtship learning in *Drosophila* is mediated by *cis*-vaccenyl acetate. *Curr Biol* 17(7):599-605.
11. Connolly K & Cook R (1973) Rejection responses by female *Drosophila-melanogaster* - their ontogeny, causality and effects upon behavior of courting male. *Behaviour* 44(1-2):142-166.
12. Dankert H, Wang L, Hoopfer ED, Anderson DJ, & Perona P (2009) Automated monitoring and analysis of social behavior in *Drosophila*. *Nat Methods*

6(4):297-303.

13. Branson K, Robie AA, Bender J, Perona P, & Dickinson MH (2009) High-throughput ethomics in large groups of *Drosophila*. *Nat Methods* 6(6):451-457.
14. Ofstad TA, Zuker CS, & Reiser MB (2011) Visual place learning in *Drosophila melanogaster*. *Nature* 474(7350):204-207.
15. Xia S, Liu L, Feng C, & Guo A (1997) Memory consolidation in *Drosophila* operant visual learning. *Learn Mem* 4(2):205-218.
16. Liu L, Wolf R, Ernst R, & Heisenberg M (1999) Context generalization in *Drosophila* visual learning requires the mushroom bodies. *Nature* 400(6746):753-756.
17. Pan Y*, et al.* (2009) Differential roles of the fan-shaped body and the ellipsoid body in *Drosophila* visual pattern memory. *Learn Mem* 16(5):289-295.
18. Zhang W, Ge W, & Wang Z (2007) A toolbox for light control of *Drosophila* behaviors through Channelrhodopsin 2-mediated photoactivation of targeted neurons. *Eur J Neurosci* 26(9):2405-2416.
19. Clyne JD & Miesenbock G (2008) Sex-specific control and tuning of the pattern generator for courtship song in *Drosophila*. *Cell* 133(2):354-363.
20. Claridge-Chang A*, et al.* (2009) Writing memories with light-addressable reinforcement circuitry. *Cell* 139(2):405-415.
21. Leifer AM, Fang-Yen C, Gershow M, Alkema MJ, & Samuel AD (2011) Optogenetic manipulation of neural activity in freely moving *Caenorhabditis elegans*. *Nat Methods* 8(2):147-152.
22. Inada K, Kohsaka H, Takasu E, Matsunaga T, & Nose A (2011) Optical dissection of neural circuits responsible for *Drosophila* larval locomotion with halorhodopsin. *PLoS One* 6(12):e29019.
23. Zhao S*, et al.* (2011) Cell type-specific channelrhodopsin-2 transgenic mice for optogenetic dissection of neural circuitry function. *Nat Methods* 8(9):745-752.
24. Kamyshev NG, Iliadi KG, & Bragina JV (1999) *Drosophila* conditioned courtship: two ways of testing memory. *Learn Mem* 6(1):1-20.
25. Keleman K, Kruttner S, Alenius M, & Dickson BJ (2007) Function of the *Drosophila* CPEB protein Orb2 in long-term courtship memory. *Nat Neurosci* 10(12):1587-1593.
26. Ishimoto H, Sakai T, & Kitamoto T (2009) Ecdysone signaling regulates the formation of long-term courtship memory in adult *Drosophila melanogaster*. *Proc Natl Acad Sci U S A* 106(15):6381-6386.
27. Fitzsimons HL & Scott MJ (2011) Genetic modulation of Rpd3 expression impairs long-term courtship memory in *Drosophila*. *PLoS One* 6(12):e29171.
28. Winbush A*, et al.* (2012) Identification of gene expression changes associated with long-term memory of courtship rejection in *Drosophila* males. *G3 (Bethesda)* 2(11):1437-1445.
29. Tully T & Quinn WG (1985) Classical conditioning and retention in normal and mutant *Drosophila melanogaster*. *J Comp Physiol A* 157(2):263-277.
30. Chen CC*, et al.* (2012) Visualizing long-term memory formation in two neurons of the *Drosophila* brain. *Science* 335(6069):678-685.
31. Card G & Dickinson MH (2008) Visually mediated motor planning in the escape response of *Drosophila*. *Curr Biol* 18(17):1300-1307.
32. Boyden ES, Zhang F, Bamberg E, Nagel G, & Deisseroth K (2005) Millisecond-timescale, genetically targeted optical control of neural activity. *Nat Neurosci* 8(9):1263-1268.
33. Zhang YP & Oertner TG (2007) Optical induction of synaptic plasticity using a light-sensitive channel. *Nat Methods* 4(2):139-141.
34. Lima SQ & Miesenbock G (2005) Remote control of behavior through genetically targeted photostimulation of neurons. *Cell* 121(1):141-152.
35. Zhang F*, et al.* (2007) Multimodal fast optical interrogation of neural circuitry. *Nature* 446(7136):633-639.
36. Han X & Boyden ES (2007) Multiple-color optical activation, silencing, and desynchronization of neural activity, with single-spike temporal resolution. *PLoS One* 2(3):e299.
37. Gradinaru V*, et al.* (2010) Molecular and cellular approaches for diversifying and extending optogenetics. *Cell* 141(1):154-165.
38. Tracey WD, Jr., Wilson RI, Laurent G, & Benzer S (2003) *painless*, a *Drosophila* gene essential for nociception. *Cell* 113(2):261-273.
39. Seelig JD & Jayaraman V (2011) Studying sensorimotor processing with physiology in behaving *Drosophila*. *Int Rev Neurobiol* 99:169-189.
40. Zhu P, Fajardo O, Shum J, Zhang Scharer YP, & Friedrich RW (2012) High-resolution optical control of spatiotemporal neuronal activity patterns in zebrafish using a digital micromirror device. *Nat Protoc* 7(7):1410-1425.
41. Suh GS*, et al.* (2007) Light activation of an innate olfactory avoidance response in *Drosophila*. *Curr Biol* 17(10):905-908.
42. Lin JY, Knutsen PM, Muller A, Kleinfeld D, & Tsien RY (2013) ReaChR: a red-shifted variant of channelrhodopsin enables deep transcranial optogenetic excitation. *Nat Neurosci* 16(10):1499-1508.
43. Inagaki HK*, et al.* (2013) Optogenetic control of *Drosophila* using a red-shifted channelrhodopsin reveals experience-dependent influences on courtship. *Nat Methods*.
44. Rafael C. Gonzalez, Richard E. Woods, *Digital image processing*, Prentice Hall, New Jersey, USA, (2008).
45. Ioannou, D., Huda, W. and Laine, A.F., Circle recognition through a 2d Hough transform and radius histogramming, *Image Vision Comput* **17**, 15-26 (1999).
46. Branson, K. *et al.*, High-throughput ethomics in large groups of *Drosophila*, *Nat Methods* **6**, 451-457 (2009).

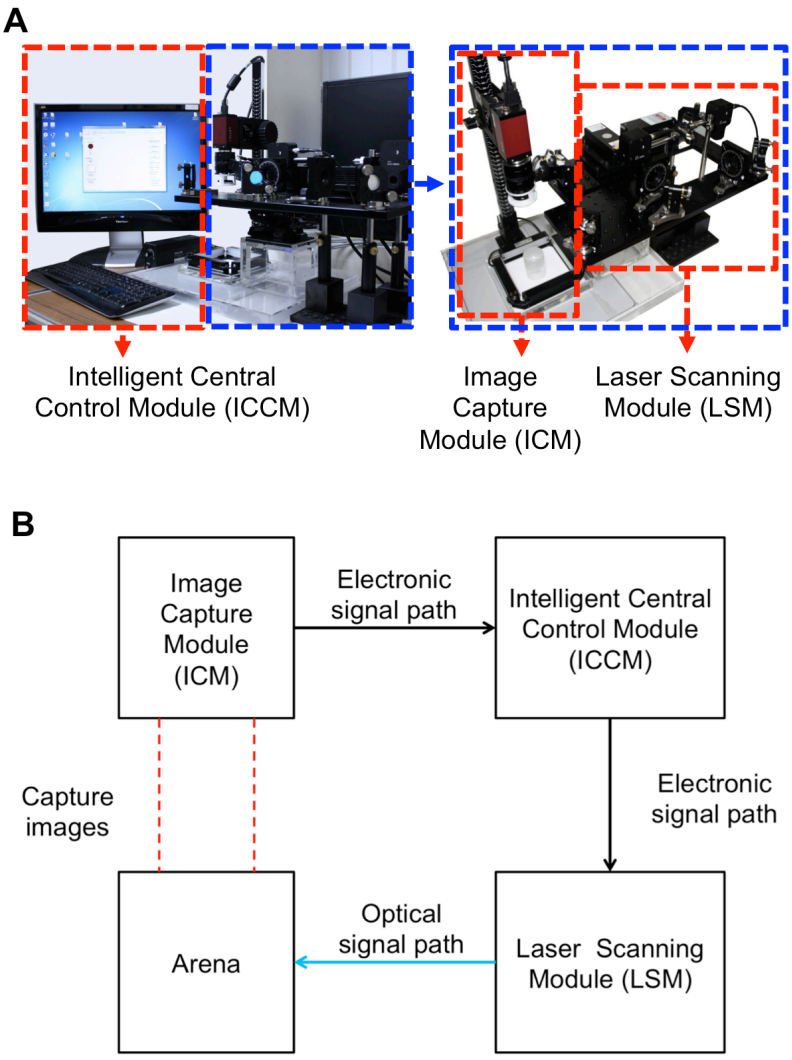

Fig. S1. ALTOMS setup. ALTOMS has four modules: an arena, an image capture module (ICM), a laser-scanning module (LSM), and an intelligent central control module (ICCM). (A) Photographs of ALTOMS. (B) Information flow among modules.

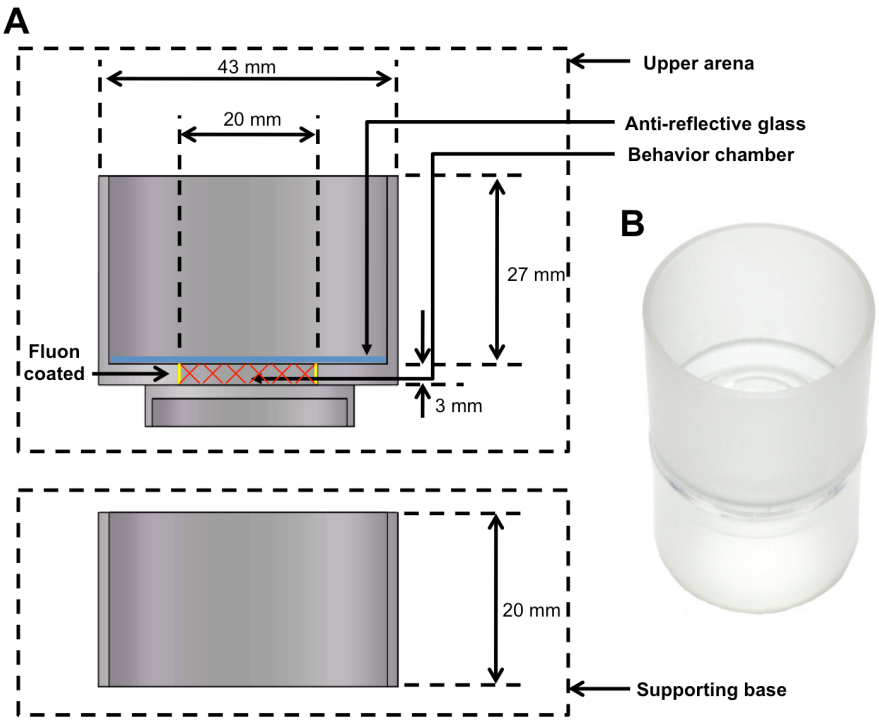

Fig. S2. Arena design. (A) The arena includes two parts: upper arena and supporting base. (B) Photograph of the arena. Most parts of the arena were made of acrylic materials. For even light illumination, we used a coarse outer surface. With regard to the behavioral chamber, the sidewall was coated with Fluon and the anti-reflective glass cover was coated with water repellent; these coatings prevented the fly from sitting on these surfaces.

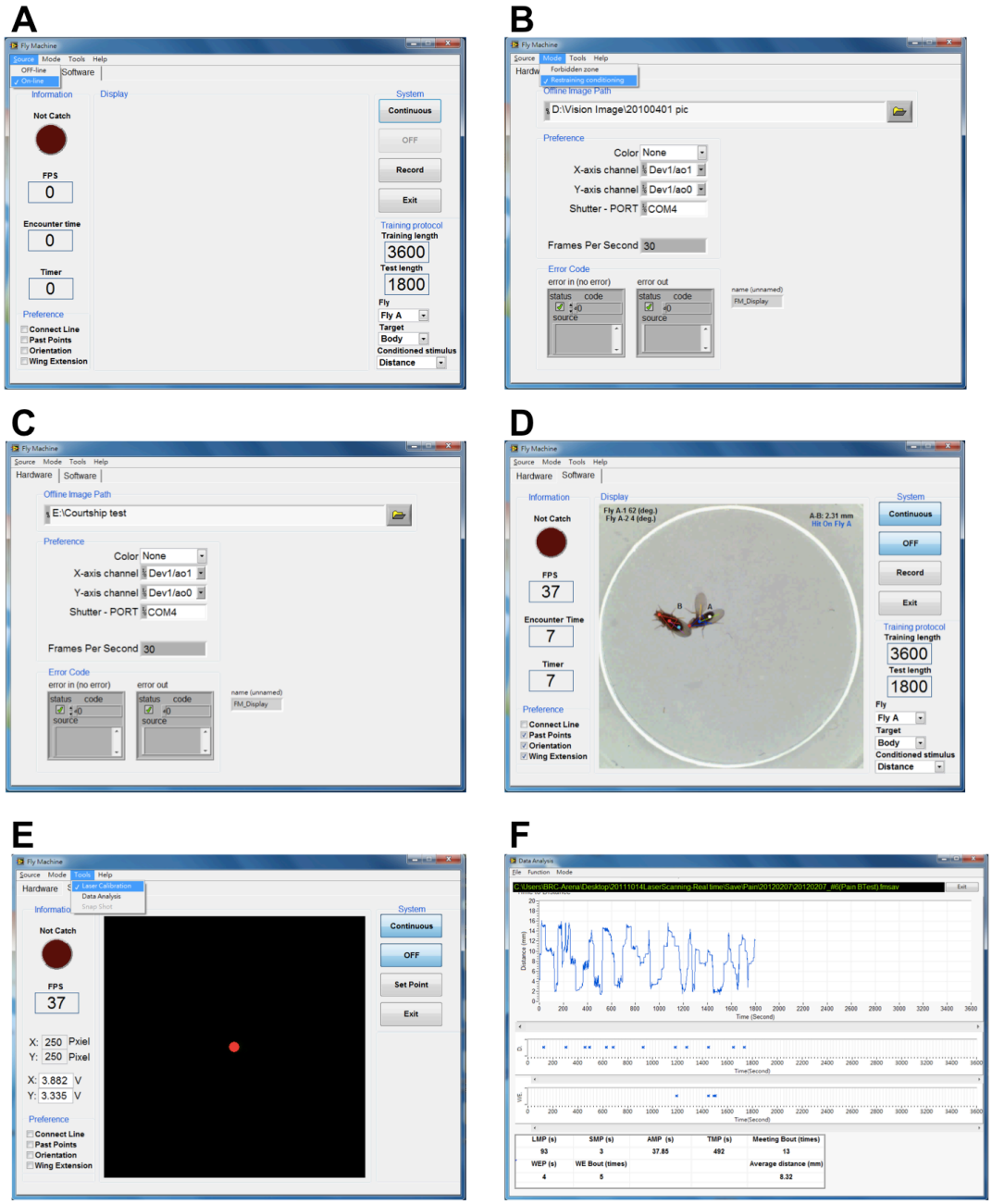

Fig. S3. Graphical user interface (GUI). (A) Source images for online/offline analysis. (B) Experimental modes: forbidden zone experiment or distance-restraining conditioning. (C) Hardware setting. (D) Software setting for distance-restraining conditioning. (E) Laser calibration tool. (F) Automated data analysis tool.

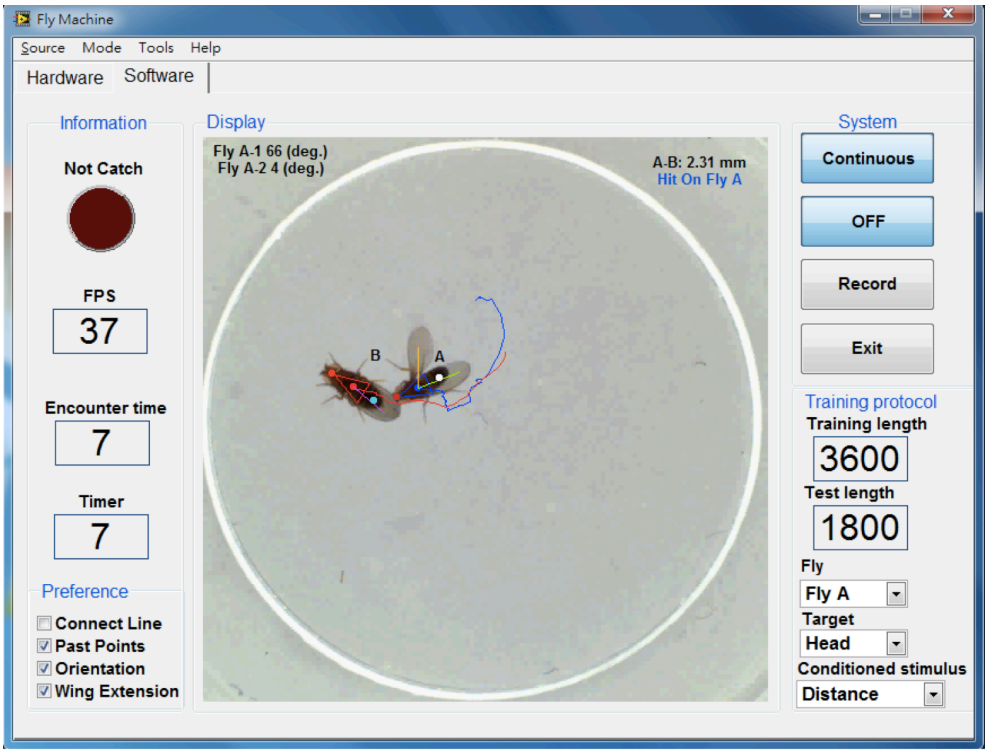

Fig. S4. Software settings for automated distance-restraining conditioning in real time. The GUI shows five functions: information, preference, display, system, and training protocol (see Supplementary Materials and Methods for details).

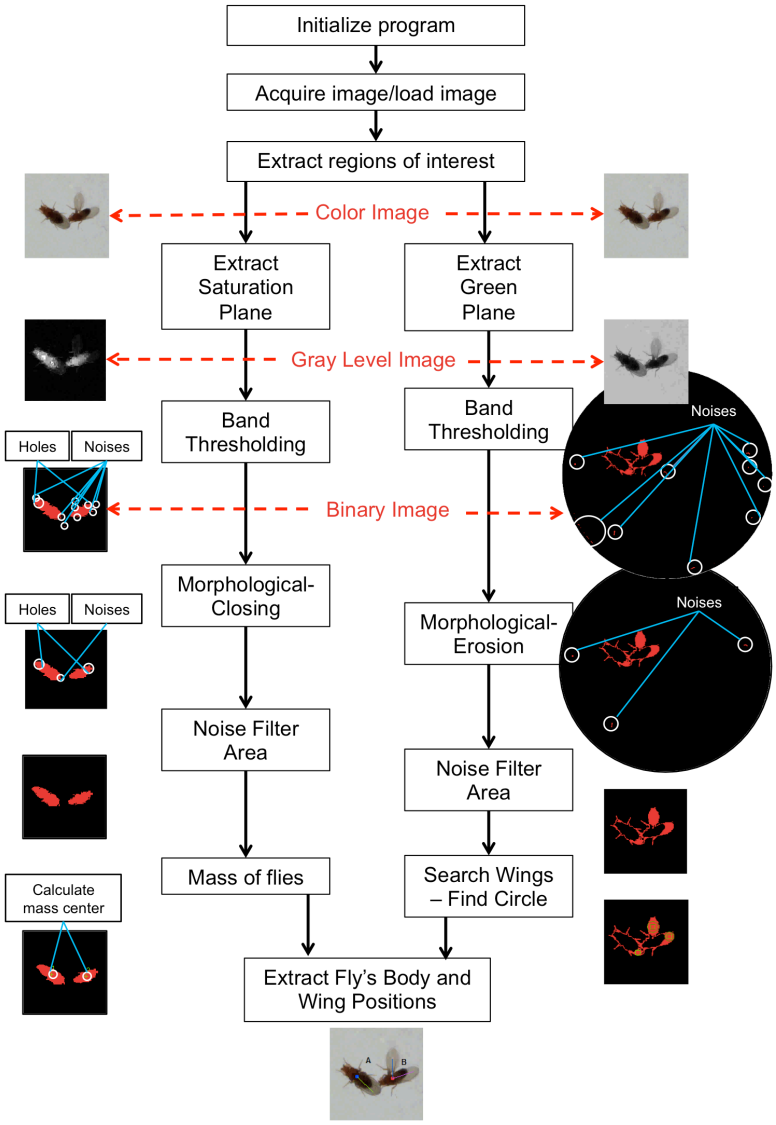

Fig. S5. Steps for parallel image processing. Left: 1) Extract the saturation plane while converting color image into gray level image. 2) Convert gray level image into binary image by using a long-pass filter. 3) Fill small holes by using "Morphological Closing" function. 4) Remove small particles by using "Area" function. 5) Calculate center of mass as an indication of fly's position. **Right:** 1) Convert color image into gray level image (green plane). 2) Convert gray level image into binary image by using a band-pass filter. 3) Remove small particles by using "Morphological Erosion" function. 4) Remove large particles by using "Noise Filter" function. 5) Identify wing positions by using "Circle Detection" function. 6) Calculate angles of wing extension from body mass center, wing mass center, and tail position. After the classifier (see Supplementary Materials and Methods), all calculated results are labeled on each fly.

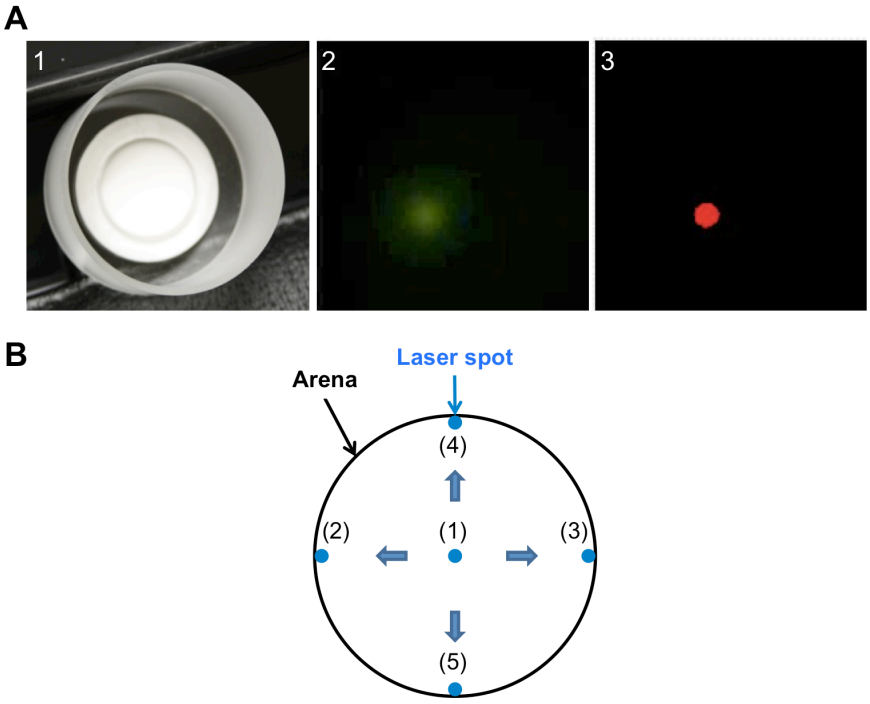

Fig. S6. Laser spot calibration. (A) A “Calibrator” arena specially designed for calibrating the laser. The bottom of the arena is made of white acrylic, which contains a fluorescent agent that fluoresces when illuminated with a blue laser. (B) Use of color threshold method for extracting laser spot from image; the center is defined by theoretical approximation.

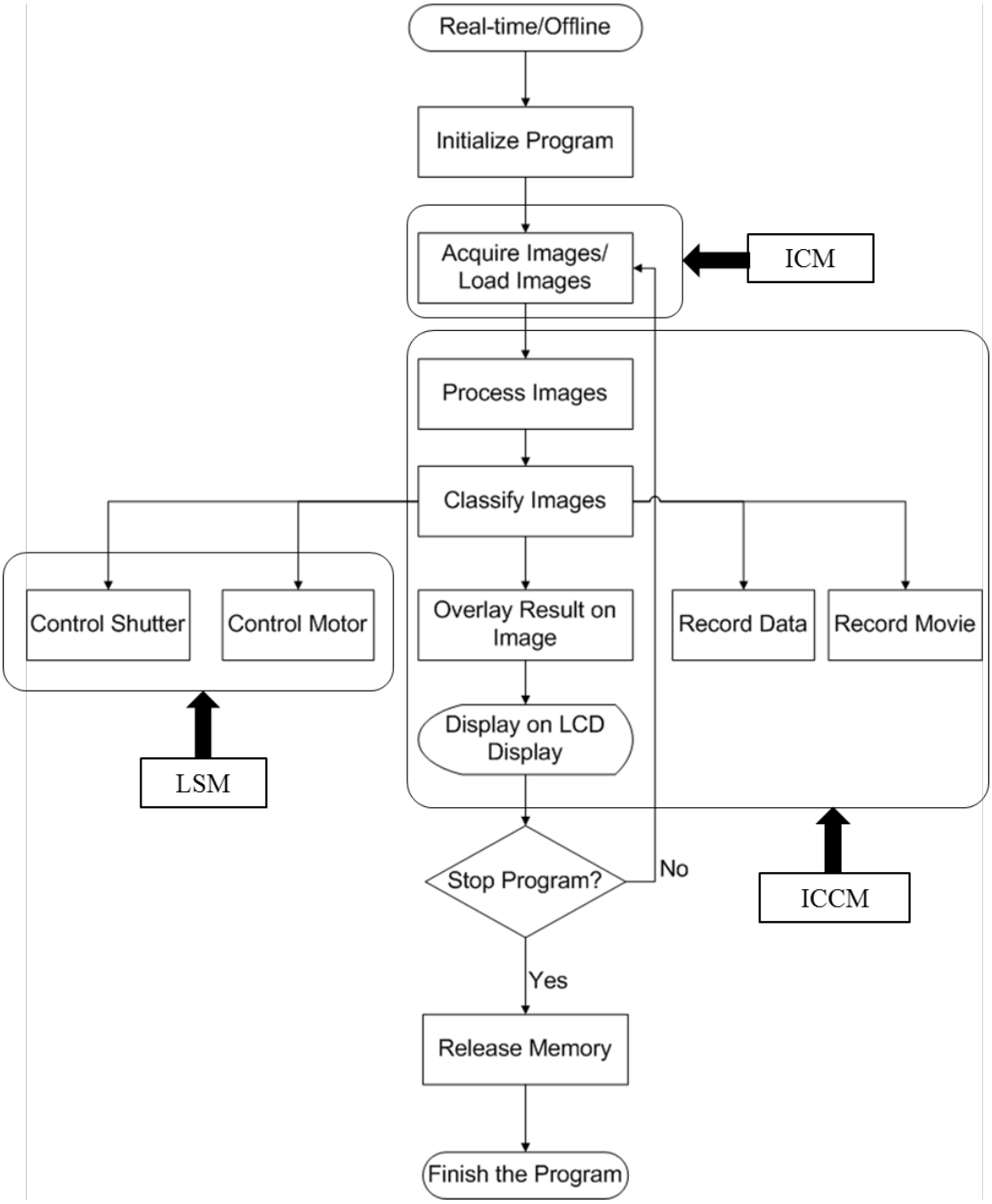

Fig. S7. ALTOMS operation flowchart

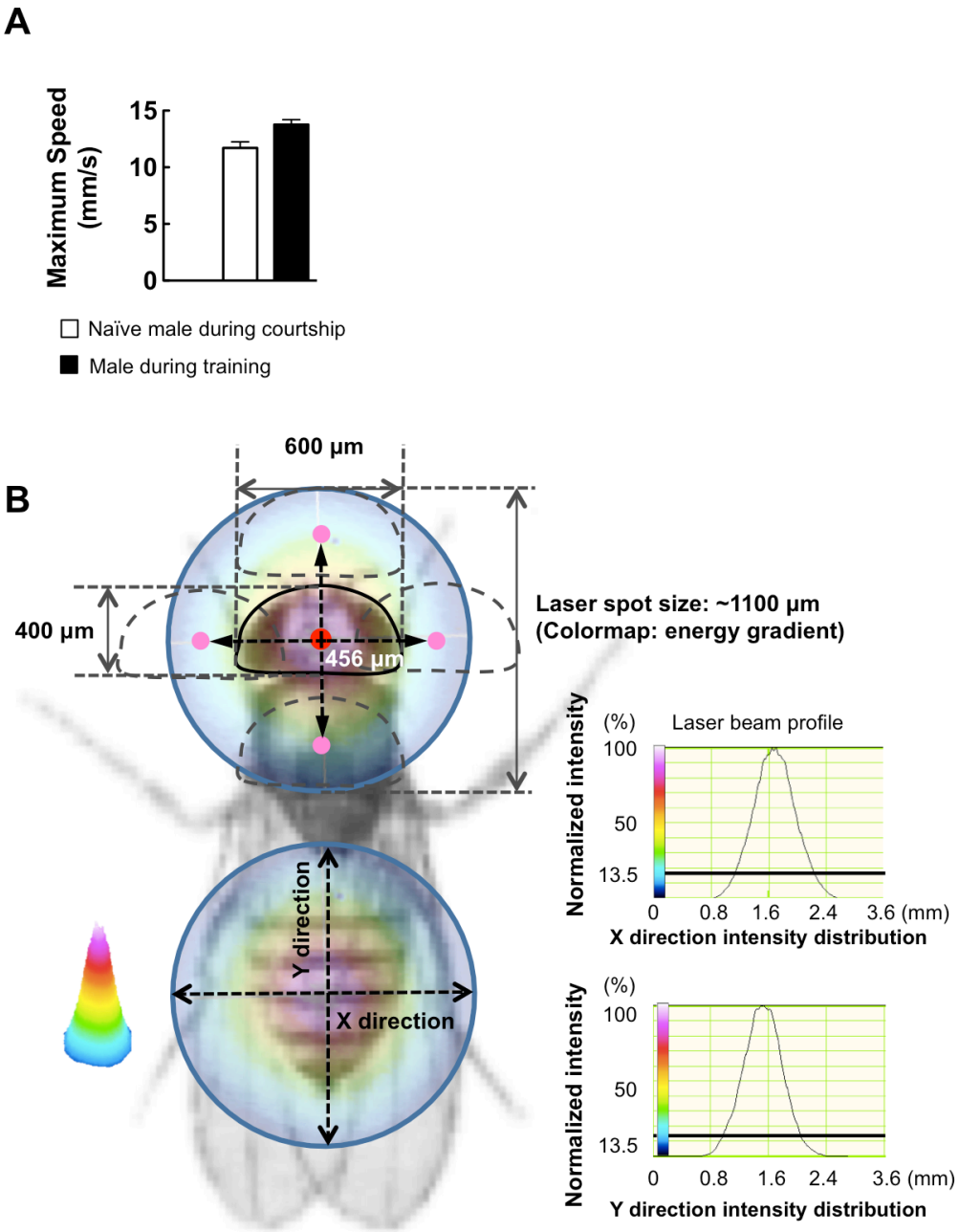

Fig. S8. Spatiotemporal precision of laser irradiation. (A) Maximum moving speed of a naïve male during courtship (white bar) and a male during distance-restraining training (black bar). Each value represents mean ± S.E.M. (n = 27). (B) Laser spot size and normalized intensity profiles. Maximum moving distance within 25 ms (maximum system delay time for online image processing) was 456 mm (average: 340 mm), which was still covered by half the laser spot size (diameter: 1100 mm). Red-to-blue color-coding within laser spot indicates high-to-low normalized intensity. Laser spot size was determined as area with >13.5% of maximum intensity.

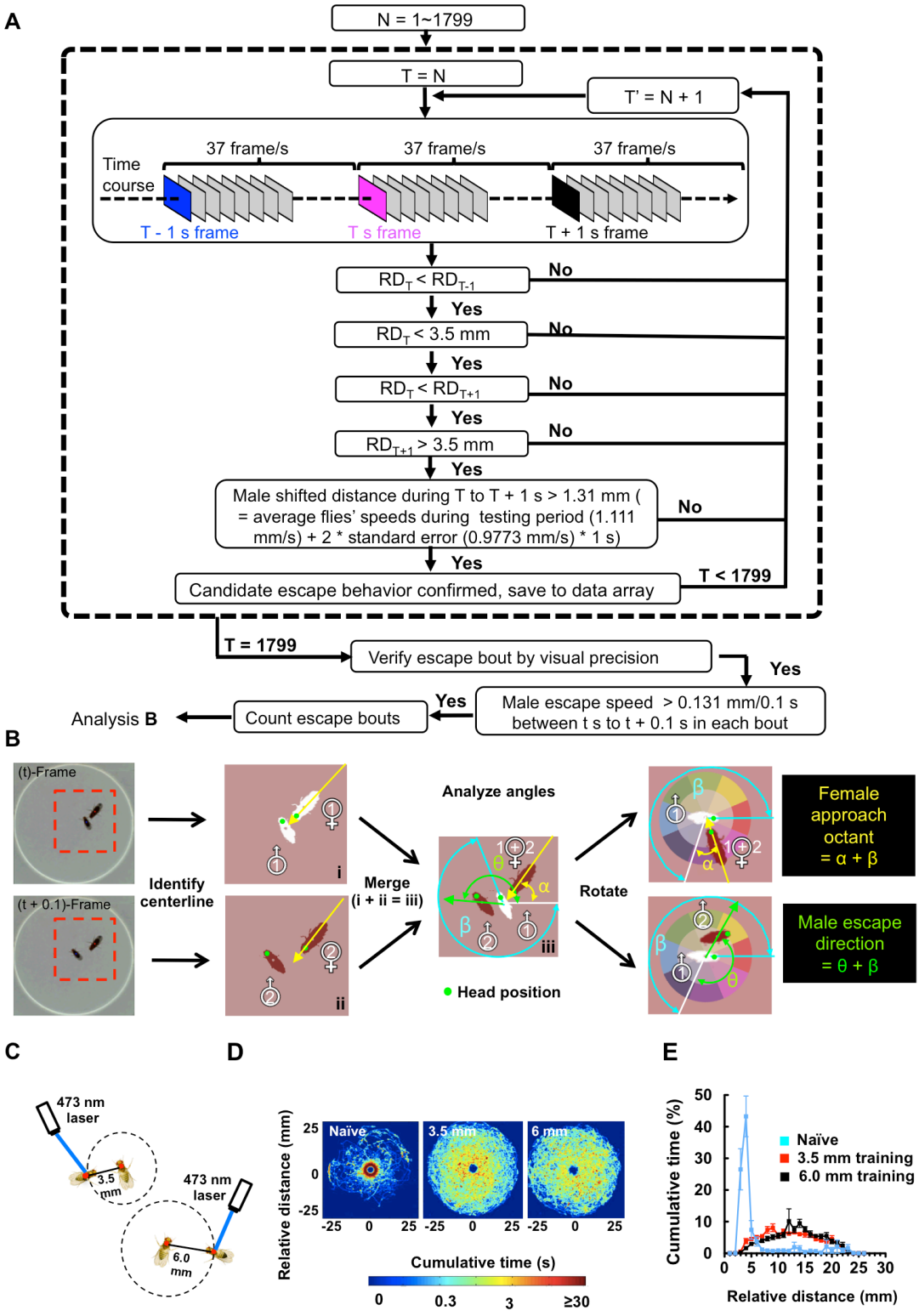

Fig. S9. Automated measurement of male escape behavior after distance-restraining conditioning. (A) Flowchart of automated selection of recorded image frames containing male escape behavior. RD: relative distance between two flies. (B) Defining female approach and male escape. α is the angle between the line connecting the center points of two flies and horizontal line. β is the angle between the long midline and horizontal line of male flies. θ is the angle between the line connecting the center points of two males from two

serial pictures (time lapse = 0.1 s) and horizontal line. To compare the escape and approach directions in the same scenario, we turned the male fly (t s) to align it with horizontal line (by plus β°) and defined the female's approach direction as α + β and male's (t + 0.1 s) escape direction as θ + β. (**C**) Conditioning at two different distances. To compare the effect of restraining conditioning at two different distances, we enlarged the arena to 25 mm in diameter. During training, we punished the male fly immediately when it met the punishment criterion (i.e., relative distance of 3.5 mm or 6 mm between two individuals). In this assay, the male was immediately punished when it met the punishment criterion to avoid confusion between 6 mm conditioning and 3.5 mm conditioning during the 2-s delay period. (**D**) Spatial distribution of a naïve wild-type male or a male trained for an hour around a freely moving virgin female during a 30-min test. The figure represents the results of 10 experiments accumulated by aligning the female's position at the center origin. Data are shown for males that are naïve or punished within 3.5 mm or 6 mm of the female. Color-coding indicates the duration for which the males stayed at a given location. (**E**) Cumulative time across different ranges of relative distance between male and female (n = 8).

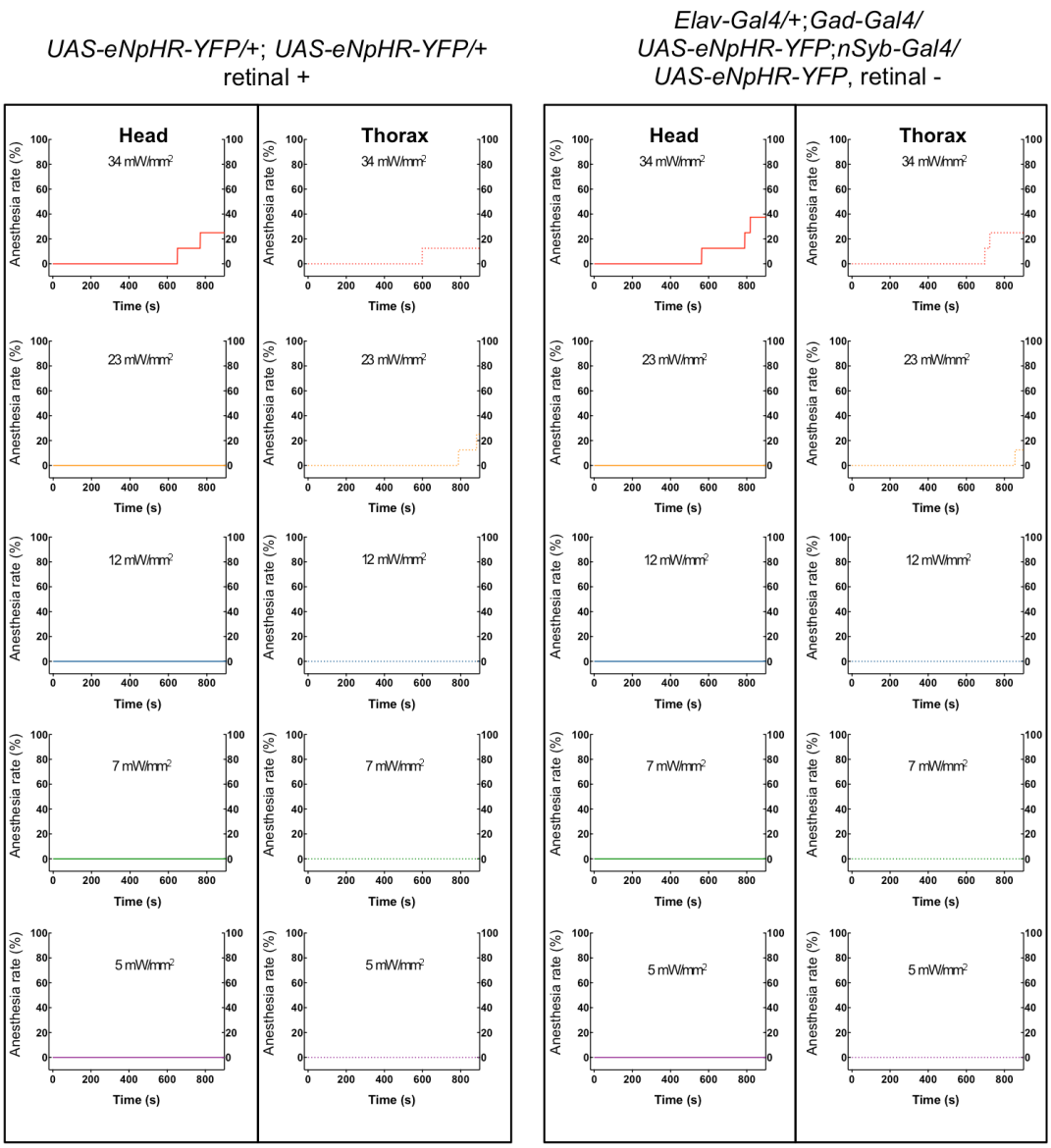

Fig. S10. Control experiments for assessing the effectiveness of laser irradiation. Fainting rate was calculated as a function of time for different laser energies. Flies carrying *UAS-eNpHR-YFP/+*;*UAS-eNpHR-YFP/+* transgenes were fed with all-*trans*-retinal for 5–7 days. Flies carrying *Elav-Gal4/+*;*Gad-Gal4/UAS-eNpHR-YFP*;*nSyb-Gal4/UAS-eNpHR-YFP* transgenes were not fed with all-*trans*-retinal.

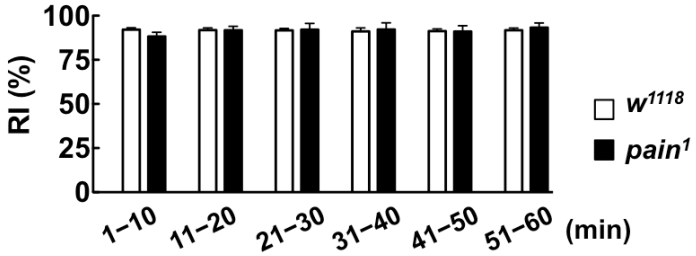

Fig. S11. Normal avoidance of *pain*^{1} mutant males during distance-restraint conditioning. Restraining index (RI) of *pain*^{1} males with laser irradiation (n = 5). Each value represents mean ± S.E.M.

Table S1. Visual validation of ALTOMS accuracy in tracking fly identities.

Assay (naïve)	Error/Frames	Error rate (%)	Assay (trained)	Error/Frames	Error rate (%)
1	1/66600	0.0015	1	1/133200	0.0008
2	0/13320	0	2	2/133200	0.0015
3	0/49469	0	3	0/133200	0
4	0/66600	0	4	0/133200	0
5	1/66600	0.0015	5	1/133200	0.0008
6	3/66600	0.0045	6	0/133200	0
7	4/29896	0.0134	7	1/133200	0.0008
8	3/66600	0.0045	8	1/133200	0.0008
Mean		0.0032			0.0006

In each assay, social interactions between a naïve male and a virgin female were continuously videotaped for 30 min or until the beginning of copulation. Trained pairs were monitored for 60 min. Videos were recorded at 40 fps. Image frames containing flies with a relative distance within 3.5 mm were automatically detected. We visually inspected the number of incidents in which ALTOMS tracked the wrong individual after crossover between two flies.